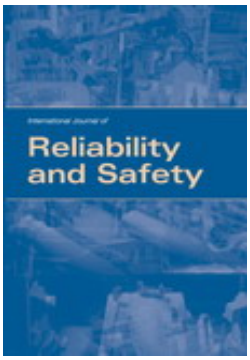

International Journal of Reliability and Safety

ISSN online: 1479-3903 - ISSN print: 1479-389X
https://www.inderscience.com/ijrs

About the reliability analysis of complex dynamical systems via fluidification: numerical approach

Hamid El-Moumen, Nabil El Akchioui, Mohammed Hassani Zerrouk

DOI: 10.1504/IJRS.2023.10057771

Article History:

Received:	01 November 2022
Last revised:	12 December 2022
Accepted:	02 February 2023
Published online:	20 August 2023

About the reliability analysis of complex dynamical systems via fluidification: numerical approach

Hamid El-Moumen*, Nabil El Akchioui and Mohammed Hassani Zerrouk

Faculty of Sciences and Technology Al Hoceima,
University Abdelmalek Essaadi,
Tétouan and Tangier, Larache, Morocco
Email: elmoumen.hmd@gmail.com
Email: n.elakchioui@uae.ac.ma
Email: m.hassani@uae.ac.ma
*Corresponding author

Abstract: The fluidification of stochastic discrete event models is a more interesting method to overcome the problem of combinatorial explosion of states. It allows to relax the conditions of stochastic Petri nets to continuous Petri nets, in order to accelerate the slow convergence of stochastic simulations. In our study, we will study an example of a large manufacturing workshop, in order to give limitations of the direct fluidification which does not always lead to the same behaviour between the two models. Secondly, we propose a numerical approach called adaptive that devotes to the adaptation of the maximum speeds of crossing the transitions that is considered as functions depending on the time. Consequently, this approach shows an excellent convergence of the continuous model to the stochastic one whatever the type of network and whatever the initial marking.

Keywords: reliability analysis; Markov model; stationary state; stochastic Petri nets; fluidification; continuous Petri nets; numerical approach.

Reference to this paper should be made as follows: El-Moumen, H., El Akchioui, N. and Zerrouk, M.H. (2023) 'About the reliability analysis of complex dynamical systems via fluidification: numerical approach', *Int. J. Reliability and Safety*, Vol. 17, No. 1, pp.1–20.

Biographical notes: Hamid El-Moumen received a master's degree in 2019, specialty, Embedded Systems and Robotics from the Faculty of Science and Technology, AL Hoceima, University Abdelmalek Esaadi of Tetouan, Morocco. He is currently a PhD student at the same faculty. His research focuses on the study of reliability, diagnosis, and monitoring of industrial facilities by continuous approaches such as Petri nets.

Nabil El Akchioui received a PhD in Automatic and Computer Science from the University of Sciences and Technologies of Le Havre in 2012, France, and an HDR from the University Abdelmalek Esaadi Tetouan, Morocco in 2020. Since 2013, he is a professor at the Faculty of Science and Technology, Al Hoceima University, Morocco. He is part of the research group in Electrical and Automatic Engineering. His research interests include Petri nets, learning processes, adaptive control, fault detection and diagnosis and its applications to electrical.

Mohammed Hassani Zerrouk holds a Master's degree in Natural Resources and Environment (in 2004) and a PhD in Water treatment (in 2007) from Cadiz

University, Spain. He was a member in the research group 'Environmental Technologies' of Cadiz University (Spain) from 2001 to 2009. Currently, he is a member of the research team: Engineering Environment, Food, and Valuation of Biomolecules of the Faculty of Sciences and Technologies Al Hoceima, University Abdelmalek Esaadi Tetouan, Morocco, where he is also a professor since 2013. His research area includes the environment and environmental technologies especially the water sector, and advanced water treatment technologies.

1 Introduction

The improvement of the reliability of industrial processes, suffers from the improvement of the study of the reliability of these processes which is presented in the systems manufactures with many interdependent elements. These studies are mainly based on stochastic models with discrete events as the Markov Chain (MC) and the Stochastic Petri Nets (SPNs) (Silva and Recalde, 2004). The analysis of the reliability is difficult to realise with MC in the systems manufactures (Vazquez et al., 2008). In this case the SPN allows under certain conditions to build equivalent models.

The MC allows to determine the probabilities of the state in particular in stationary regime and to calculate the usual indicators of the reliability of the systems (Vazquez et al., 2008; Navarro-Gutiérrez et al., 2022). This method allows an analytical solution of the stationary state of a SPN, which makes it valid only in systems of reduced dimensions (Silva and Recalde, 2004; Arzola et al., 2020). When systems become more complex, the SPN can be seen as an estimator of the MC. Among the SPNs extensions, the SPN with random transition time (Navarro-Gutiérrez et al., 2016). The marking of the Petri Net (PN) is then a homogeneous Markov process (Lefebvre, 2014; El-Moumen et al., 2022), moreover, the random behaviour of the SPN is identical to that of the MC. So for any SPN we can associate a homogeneous MC.

SPNs present a major difficulty because of the combinatorial state explosion problem (Vazquez and Silva, 2009), this difficulty is the speed of convergence of the state probabilities in the stationary state of the SPN. To overcome this problem, Continuous Petri Nets (CPNs) are developed in order to find continuous approximations of discrete PN (Giua and Silva, 2018), i.e., to transform the SPN into a CPN by a method called fluidification (Lefebvre, 2011; Silva and Recalde, 2004). The fluidification of SPNs gives unlikely results for which the structural and behavioural properties are not identical (El Akchioui, 2017). In detail, a PN can be alive as a discrete and non-liveness after fluidification and a discretised bounded system can be non-boundary after fluidification (Vazquez et al., 2008). The average flow of the CPN is not always an upper bound on that of the SPN (Lefebvre, 2011). Some results exist for finding stationary state majors for CPN and for SPN by solving linear programming problems (Silva and Recalde, 2004; Giua and Silva, 2018). But there is no comparison between the two obtained majors (discrete and continuous). For SPN, the equilibrium points cannot be directly approximated by those of CPN. Specifically, direct fluidification under the semantics of infinite server does not lead to the same behaviour. The average markings and asymptotic average flows of SPN and CPN with the similar structure and similar initial marking are not identical in the general case. In this context, our work continues to approximate these two models, in order to reach the same behaviour. We propose to fluidify the SPN and CPN by an adaptive approach, which consists in adopting all the maximum speeds of

crossing transitions by a corrective factor considered as a function of time, so that the modified CPN converges to the stochastic model whatever the type of network and whatever the initial marking.

The paper is organised in four sections. Section 2 presents the basic definitions of PN, SPN and CPN as well as discussions on the limitations of using SPN. Section 3 provides an example of implementing a complex manufacturing system to deal with the SPN bounds according to a CPN through direct fluidification by dealing with different cases of initial marking to show that this method is not applicable when the initial marking increases and when of the existence of many regions. Moreover, we will introduce a new semantics, the adaptive approach, by modifying the timed continuous crossing rates of the PNs to have the convergence independently of the initial marking. The last Section 4 gives some conclusions.

2 Stochastic and continuous petri nets

2.1 Petri nets (PN)

A PN is a mathematical model used to represent various systems operating on discrete variables. It is a bipartite directed graph that has places and transitions as its two types of vertices (Vazquez and Silva, 2009). A place is symbolised by a circle and a transition by a line. The finite set of n places is represented by $P = \left[P_1, P_2, ..., P_i\right]$ and the finite set of q transitions, $T = \left[T_1, T_2, ..., T_q\right]$, results in a change in the state of the system (Giua and Silva, 2018). Each P_i and T_j is linked by arcs which connect either a P_i to a T_j, or a T_j to a P_i (Lefebvre, 2011). According to the backward and forward incidence applications. We denote the forward incidence application $W^{PR} = \left(w_{ij}{}^{PR}\right) \in IN^{n\times q}$ where $w_{ij}{}^{PR}$ is used to indicate the weight of the arc directed from P_i to T_j, and the backward incidence application $W^{PO} = \left(\ w_{ij}{}^{PO}\right) \in IN^{n\times q}$ (El Akchioui, 2017) where $w_{ij}{}^{PO}$ is used to indicate the weight of the arc directed from T_j to P_i (Giua and Silva, 2018). $W = \left(W^{PO} - W^{PR}\right) \in Z^{n\times q}$ denotes the network incidence matrix (Giua and Silva, 2018). PN is characterised by the marking vector at time $t = 0$ and the marking vector at time *t* represented, respectively by M_1 and $M(t)$. $M(t)$ is an application from the set of places to the set of natural numbers (Campos et al., 1991), $M(t)$ is a column vector that represents the number of marks (or tokens) present in every place. The marking of the place P_i will be noted $M(P_i)$, or more succinctly m_i. Every transition T_j is triggered depending on its degree of activation $n_j\left(M(t)\right)$ which is determined for the marking $M(t)$ according to equation (1) (Campos et al., 1991):

$$\text{For all } P_i \in {}^{\circ}T_j,\ n_j(M) = \min\left(\ M(P_i)/w^{PR}{}_{ij}\right) \tag{1}$$

The crossing of a transition T_j can only be done if each place upstream $\left(T_j\right)$ of this transition contains at least several marks equal to the weight of the arc connecting this

place to T_j. This transition will then be validated (David and Alla, 1992) and can be crossed, allowing the evolution of the network towards a new state (Molloy, 1981).

2.2 Stochastic petri nets (SPN)

SPNs are tools for analysing the structure and behaviour of stochastic discrete event dynamical systems (Vazquez and Silva, 2009). They are timed PNs with transition firing times randomly distributed according to an exponential probability distribution with a parameter that varies $round\left(n_j\left(M\right)\right).m_i$ (Lefebvre, 2011). Molloy was the first to introduce this model (David and Alla, 1992; Molloy, 1981) and several other expansions have been developed for the analysis of the reliability of repairable systems (El Akchioui, 2017). Fundamentally, a $SPN =< PN, \mu >$, with $\mu = \left(\mu_j\right) \in \left(R^+\right)^q$ is a vector of crossing rate. The crossing rate μ_j characterises each T_j such that $\left(\mu j.dt\right)$ is the estimated probability of crossing T_j at a time (t) and $\left(t + dt\right)$ when T_j has been crossed, with an activation degree equal to 1 at time t. The characteristics of an SPN, such as incidence matrices, firing rates, initial marking and policy compliance (firing, servers and execution), are all used to describe the process of marking of an SPN (Mahulea et al., 2008; El Akchioui, 2017). The vector of the average flow and average marking of an SPN at time t will be named $X_s\left(t\right)$ and $M_s\left(t\right)$ (Campos et al., 1991). The SPNs in this work have satisfied the hypotheses (A_1) to (A_5) (El Akchioui, 2017):

- (A_1) the marked SPNs are bounded.
- (A_2) the marked SPNs can be reset.
- (A_3) the firing policy is based on the race: the transition that is assumed to be the one that will be triggered next.
- (A_4) the server policy is based on the infinite server type: influence of the degree of crossing.
- (A_5) the execution policy is based on memory resampling: influence of the transition crossed on the next crossings.

Therefore, the SPNs considered have an accessibility graph $A\left(SPN, M_I\right)$ with finite states and their marking process is represented in a MC with a state space isomorphic to $A\left(SPN, M_I\right)$ (Lefebvre et al., 2010, 2009). In this situation, the asymptotic behaviour of SPN can be computed in terms of the probability of the stationary state of the MC (El-Moumen et al., 2022).

For living SPNs that satisfy the above assumptions and when the state space is finite, the SPN has a marking graph that is isomorphic to the state space of a MC (Molloy, 1982). In this case, the Stationary state of the SPN can be deduced from the state probabilities of the MC (Molloy, 1982). The vector of Stationary state probabilities which is the solution of equation (2), is given by Lefebvre (2011):

$$\Pi_{SS}.A\left(\mu\right) = 0 \text{ and } \Pi_{SS}.1_N = 1 \tag{2}$$

With $\Pi_{SS} = (\pi_{ssk}) \in [0,\ 1]^{1\times N}$ as the vector of stationary state probabilities of the MC associated with *N* states. $A(\mu) \in (R)^{N\times N}$ as the MC generator associated with the SPN is a square matrix of dimension $N \times N$, *N* being the finite number of states of the linked MC and $1_N = (1,\ldots,1)^T \in (R^+)^N$ represents a vector of dimension *N* whose all components are equal to *1*.

Let $X_s = (x_{sj}) \in (R^+)^q$ represent the average flow vector and $M_s = (m_{si}) \in (R^+)^n$ represent the average SPN markings vector (Bobbio et al., 1998). As a consequence, from the vector Π_{SS}, we will deduce the average flows of transitions as well as the average markings of places as shown in equations (3) and (4).

$$x_{sj} = \mu_j . \left(\sum_{k=1\ldots N} n_j (M_k) . \pi_k \right) \tag{3}$$

$$m_{si} = \sum_{k=1\ldots N} m_{ki} . \pi_k \tag{4}$$

$M_k = (m_{ki}) \in (R^+)^n$ signifies the vector of marking corresponding to the state *k* of the MC (Bobbio et al., 1998). When it comes to ergodic MC, This method yields an analytical solution to the SPN stationary state, but it necessitates the computation of the transition matrix $A(\mu)$ (Silva and Recalde, 2002), as a result, the SPNs accessibility graph $A(PN, M_I)$ is isomorphic to the MC (Lefebvre et al., 2010). *N* As the number of states, rises exponentially, for large system dimension the calculation time and memory needs to evaluate $A(PN, M_I)$ becomes more relevant. In this case, for the MC, SPN can be thought of as a stochastic estimator. The benefit of this estimator is that it eliminates the need to determine $A(PN, M_I)$, but, the stochastic estimator is slow to converge, especially for rare events (El-Moumen et al., 2023).

2.3 SPNs algorithm

The simulation of stochastic systems allows the determination of estimates of indicators related to operational safety, such as reliability, mean time to failure state or availability. For large systems, Markov analysis is often unpractical due to the combinatorial explosion caused by the state graph (El Akchioui et al., 2020; Rausand and Hoyland, 2004). The simulation of SPNs does not require the calculation of the state graph and the SPNs can be thought of as an estimator of the MC.

The algorithm of the stochastic estimator, which makes it possible to determine the stationary state and compare the random behaviour of the SPN with that of a homogeneous MC and has a finite state space, is as follows Figure 1.

2.4 Complexity of the reachability graph

As an example, we will consider the example prepared by Navarro-Gutiérrez et al. (2022) presented in Figure 2. This network models a manufacturing system with 5 machinery (T_1 to T_5), and 3 resources limited tools (P_1 to P_3). In this PN model, the vector of

the parameters of the transitions μ and the initial marking M_1 are given by: $\mu = (1,1,1,1,1)^T$, $M_1 = (6k, 6k4k, 0, 3k, 0, 3k, 0, 0)^T$ where $k \in IN$.

Figure 1 Steady state by SPNs algorithm

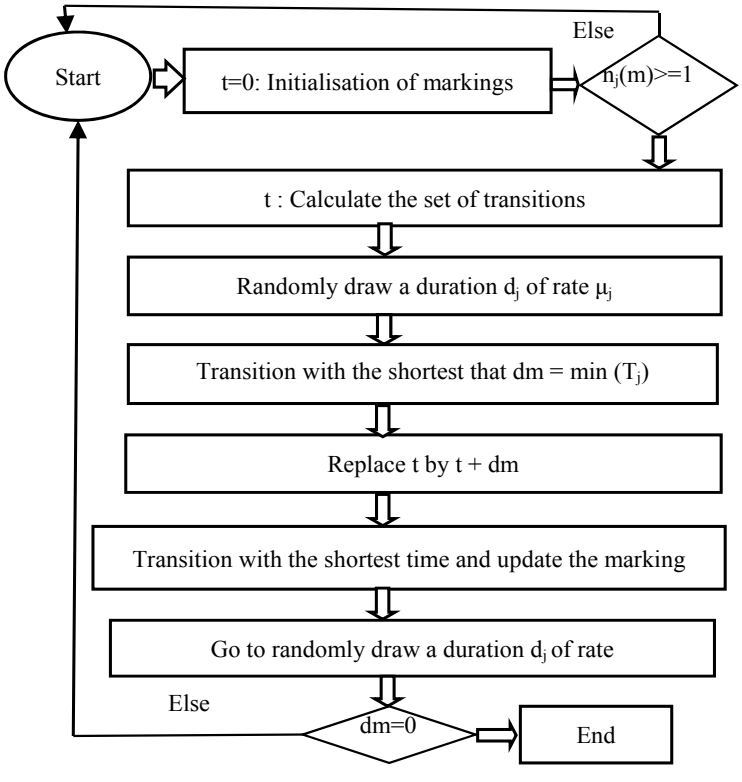

Figure 2 Manufacturing system (Silva and Recalde, 2004)

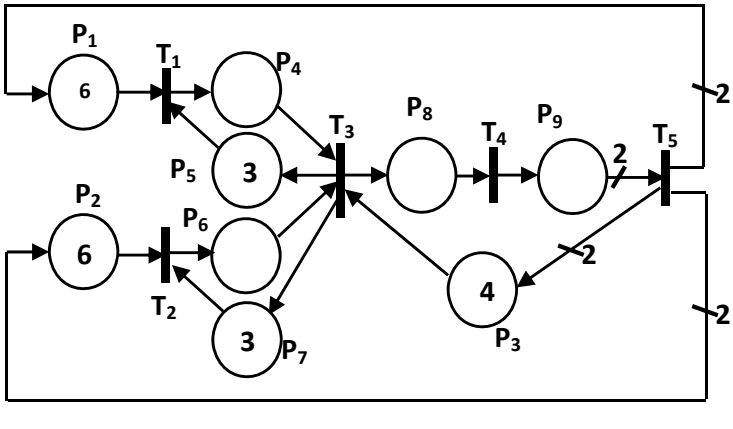

Table 1 illustrates the evolution of the number of states *N* and of the computation time as a function of the parameter *k*. the computational time required to compute the $A(PN, M_I)$ increases exponentially and makes Markov analysis difficult if not impossible (El-Moumen et al., 2022; Bobbio et al., 1998).

Table 1 Number of states and calculation time of the reachability graph depending on *k*

Coefficient k	*1*	*2*	*3*	*4*	*5*
Number of states (N)	205	1885	7796	22187	50801
Calculation time (s)	0.113	8.304	164.665	1321.804	6959.09

We have seen that for large-dimensional systems, the Markov analysis is often unpractical because of the combinatorial explosion due to the passage through the state graph (Silva and Recalde, 2002; El Akchioui et al., 2020). The simulation of the SPNs does not require the computation of the state graph and the SPNs can be considered as an estimator of the MC (Rausand and Hoyland, 2004; Júlvez et al., 2005). The advantage of this estimator is that the determination of $A(PN, M_I)$ is no more necessary, the drawback is the slow convergence of the stochastic estimator, particularly in the case of rare events (Rausand and Hoyland, 2004).

To work around this problem, we will use the link between SPNs and CPNs to estimate the main markings and average flows from the simulation.

2.5 Continuous petri nets and regions in the reachability space

Timed Continuous Petri Net (TCPN) is an expansion of a discrete timed PN on the transitions (Benaya et al., 2018). TCPNs have been used to approach the average behaviour of SPNs (Navarro-Gutiérrez et al., 2016; Lefebvre and Hadjicostis, 2022). $CPNs < PNs, X_{\max} >$ Where $X_{\max} = diag\left(x_{\max j}\right) \in \left(R^+\right)^{q*q}$ the matrix diagonal of maximum speeds. Let be $M_c(t) \in \left(R^+\right)^n$ the vector of continuous markings $m_{ci}(t)$ of places P_i. Let be $X_c(t) \in \left(R^+\right)^q$ the vector of continuous speeds of transitions T_j. $M_c(t) \in \left(R^+\right)^n$ the evolution of the marking is provided by equation (5) (El-Moumen et al., 2022):

$$dM_c(t)/dt = W.X_c(t), M_c(0) = M_I \tag{5}$$

The equation governing the instantaneous velocity of the transition is given by El-Moumen et al. (2022).

$$x_{cj}(t) = x_{\max j}.n_j\left(M_c(t)\right) \tag{6}$$

The notion of region appears because of the ' $\min(.)$ ' function in the activation degree expression. The marking area is separated into *k* regions A_k (Vazquez and Silva, 2009) (some regions may remain empty). Every A_k is characterised by its combination (configuration) (Silva and Recalde, 2002), also referred $PT - sum(A_k) = \left\{\left(P_i, T_j\right)\right\}$

(Lefebvre et al., 2015; Benaya et al., 2019). In this way P_i is the critical place of T_j in A_k (Júlvez et al., 2005). The number of configurations is related to the number of synchronisations as well as the number of places upstream of the synchronisation transitions: $K = \left|{}^{\circ}T_1\right| x \ldots x \left|{}^{\circ}T_q\right|. PT - sum\left(A_k\right)$ is defined as the sum of all combinations $\left(P_i, T_j\right)$, $j = 1,..,q$, defined by equation (7).

$$PT - sum\left(A_k\right) = [\left(P_i, T_j\right) s.m. \forall M_c\left(t\right) \in A_k, x_{cj}\left(t\right) = x_{maxj}\left(t\right).m_{ci}\left(t\right) / w_{ij}^{PR}] \quad (7)$$

Each A_k region is identified by a matrix constraint $A_k = \left(a_{ij}{}^{k}\right) \in \left(R^{+}\right)^{q \times n}$, $i = 1,...,q$, $k = 1,\ldots,K$ and $j = 1,...,n$:

- for all $T_j \in T$, $a_{ji}{}^{k}\left(k, j\right) = 1 / w_{i(k,j)j}{}^{PR}$,
- Otherwise, $a_{ji}{}^{k} = 0$.

Consequently, in every A_k, the maximal crossing speeds vector may be given by $X_c\left(t\right) = X_{max}. A_k. M_c\left(t\right)$, equation (8) is verified:

$$dM_c\left(t\right)/dt = W. X_{max}. A_k. M_c\left(t\right), \forall M_c\left(t\right) \in A_k \quad (8)$$

3 Approximation of SPN by TCPNs

In this section, we will present an example of manufacturing system, in order to study the direct total fluidification of SPNs, we will show that this last method does not always lead to a continuous behaviour identical to that of the stochastic. Furthermore, we will introduce and apply the procedure of the adaptive approach, which will allow us to obtain a continuous asymptotic regime converging to the stochastic one.

3.1 Case study: production system

Let us consider the system sketched in Figure 3, which models a complex manufacturing system. The final products is composed of two different parts consisting of two ranges of tool products, any range includes two machines M_1, M_2 and a stock (at finite capacity). The first range processes the products by the M_1, and then by the M_2, on the other hand the parts are treated in the first stage in the second range by the M_2, then in the second stage by the M_1. Each product has a single operation at each machine and pallets, which will be reused at each end of the production cycle, transport the products. This process is characterised by the presence of at least one assembly module (a convergence of flows) which requires two input components. For example, in Figure 3, product $A + B$ is assembled from A and B via M_3.

Figure 3 Assembly workshop for two product lines

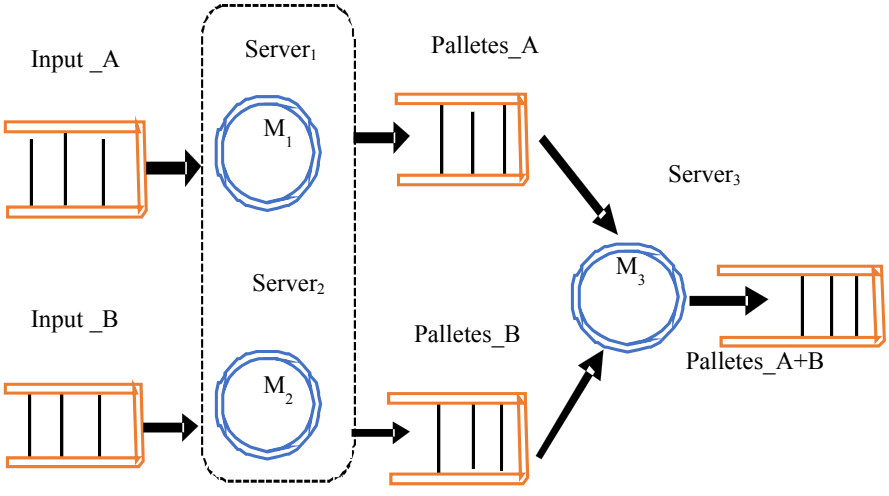

3.2 Modelling the production system

After having described the production system from a structural point of view, we are interested in obtaining a model representing it. The latter is essential for the analysis of behaviour and performance in the simulation. The system is modelled by a SPN of Figure 4 whose crossing rates of all the transitions are supposed equal to 1 (the average duration of each elementary operation is 1) and of initial marking $M_I = (35\ 0\ 0\ 0\ 10\ 1\ 1\ 25\ 0\ 0\ 0\ 10\ 1\ 1\ 1\ 0\ 25\ 0)^T$.

The system in Figure 4 is composed of two different parts A and B. Part A is processed in M_1 and then M_2, respectively, while part B is processed in M_2 and then in M_1. The intermediate products are stored in places B_1_A and B_1_B and the final products, respectively in places B_2A and B_2B. The M_3 brings together the parts A and the parts B producing final parts. In this system, we have three sequential machines, four intermediate depots and a terminal depot. Initially, there are 35 type A pallets (M_1 (*Pallets_A*)= 35), 25 type B pallets (M_1 (*Pallets_B*) = 25), one machine of each type from which the first two are initially at rest, while the third is the working state $(M_I(M_1\_Iddle) = M_I(M_2\_Iddle) = M_I(M_3\_Work) = 1)$, only one type A final product and another type B product $(M_I(B\_2A) = M_I(B\_2B) = 1)$. The maximum A and B type coins that can be produced each time is 10 $(M_I(\text{Max}\_A) = M_I(\text{Max}\_B) = 10)$. The final product is stored in place *B_3* and the parts are moved on the two pallets. Finally, the memory capacity to store the finished products just before recycling the pallets is equal to 25 $(M_I(B\_3\_Empty) = 25)$.

Figure 4 Model of complex manufacturing system

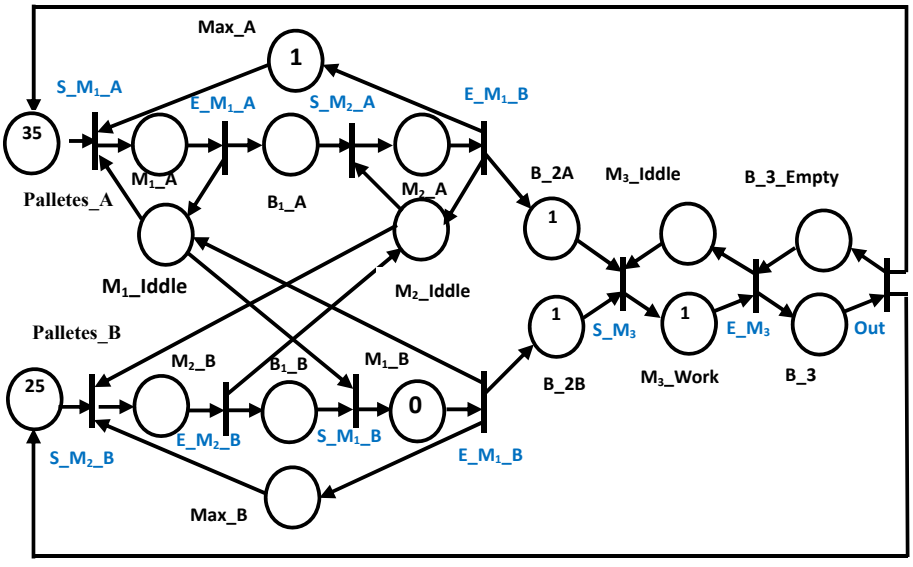

3.3 *Direct fluidification of SPN*

The SPN presents a major problem of combinatorial explosion of the number of states which is inherent in high-dimensional discrete event systems. Increasing the size of the reachability graph of discrete systems is a complex problem. It is therefore important to simplify the study of systems for their analysis and verification. One possible approach is the transition from a discrete event system to a continuous system. This is called fluidification. It is considered as an approximation technique allowing to analyse a system at a lower cost, i.e., with a significant decrease of the computing resources (El Akchioui, 2017; Lefebvre, 2004; Silva and Recalde, 2002).

Consider the SPN model of the stochastic production system described in Figure 4 (Silva and Recalde, 2002), with initial marking $M_I = (35\ 0\ 0\ 0\ 10\ 1\ 1\ 25\ 0\ 0\ 0\ 10\ 1\ 1\ 1\ 0\ 25\ 0)^T$ and of crossing rate $\mu = (1\ 1\ 1\ 1\ 1\ 1\ 1\ 1\ 1\ 1\ 1)^T$. This system is defined by a single firing invariant T-semi flow $z_1 = (1\ 1\ 1\ 1\ 1\ 1\ 1\ 1\ 1\ 1\ 1)^T$ and eight marking invariants defined by the P-semi flows $(Y_1\ Y_2\ Y_3\ Y_4\ Y_5\ Y_6\ Y_7\ Y_8)^T$. We will study the direct fluidification of the stochastic model of Figure 4 for different values of the initial marking in order to compare. This approximation turns out to be the best solution for this large system and its rather large initial marking. To illustrate the results, we present the evolution of the stochastic and continuous marking of the $B-2A$ place, as well as the stochastic and continuous flow of the *Out* transition for different initial markings.

Figures 5 and 6 present, respectively, the evolution of the continuous and stochastic flow of the Out transition and the continuous and stochastic marking of the $B-2A$ place for an initial marking $M_I = (3\ 0\ 0\ 0\ 1\ 1\ 1\ 2\ 0\ 0\ 0\ 1\ 1\ 1\ 1\ 0\ 2\ 0)^T$.

Figure 5 Flow evolution of CPN and SPN for transition *Out* in function of time of Figure 4

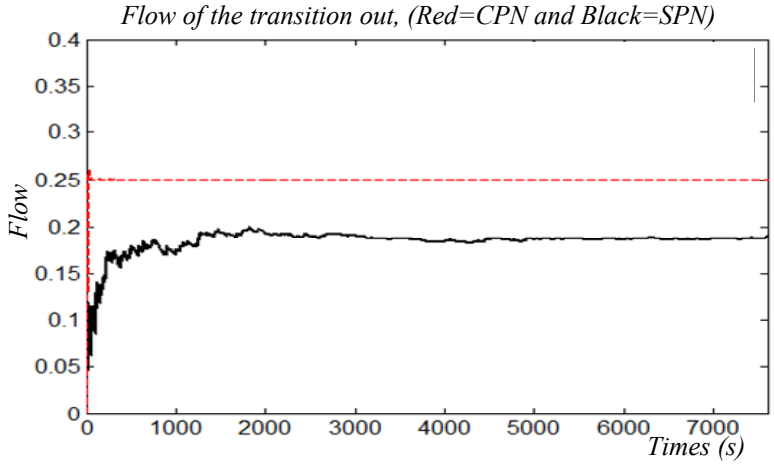

Figure 6 Marking evolution of CPN and SPN for place $B-2A$ in function of time of Figure 4

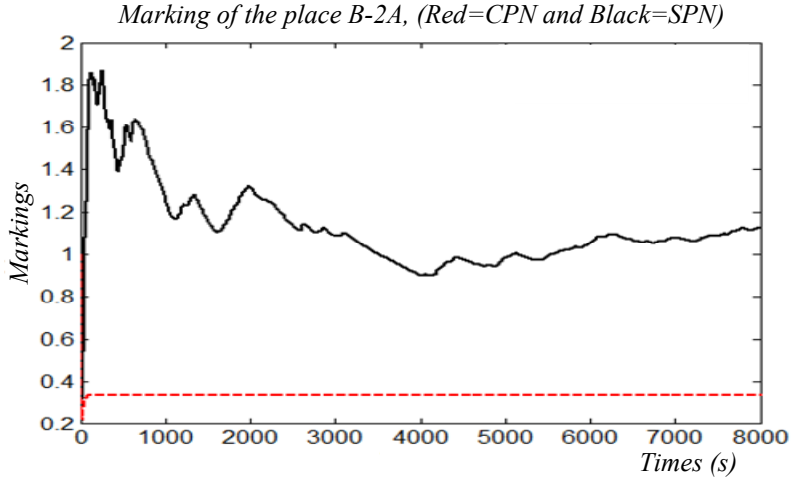

Table 2 gathers the results obtained by the direct fluidification of the stochastic system of Figure 4 of the continuous and stochastic marking of the place $B-2A$ and of the continuous and stochastic flow of the *Out* transition.

Table 2 Average flows and average markings of CPN and SPN from Figure 4

$M_I = (3\ 0\ 0\ 0\ 1\ 1\ 1\ 2\ 0\ 0\ 0\ 1\ 1\ 1\ 1\ 0\ 2\ 0)^T$	*SPN*	*CPN*	*Error*
Flows	0.193	0.25	0.29
Average markings	1.1585	0.25	0.78

From the simulation, presented in Figures 5 and 6, we can see that the behaviour of TCPN obtained by the direct fluidification of the SPN with the same initial marking

$M_1 = (3\ 0\ 0\ 0\ 1\ 1\ 1\ 2\ 0\ 0\ 0\ 1\ 1\ 1\ 1\ 0\ 2\ 0)^T$ does not converge to stochastic behaviour. In the second case, we will increase the number of marks circulating in the system. For this, we chose the initial marking $M_1 = (7\ 0\ 0\ 0\ 2\ 1\ 1\ 5\ 0\ 0\ 0\ 2\ 1\ 1\ 1\ 0\ 5\ 0)^T$. The results of the total direct fluidification of the system are shown in Figures 7 and 8, where Figure 7 represents the evolution of the CPN and SPN marking of the place $B - 2A$ and Figure 8 illustrates the CPN and SPN Evolution of the flow of the *Out* transition as a function of time.

Figure 7 Marking evolution of CPN and SPN for place $B - 2A$ in function of time of Figure 4

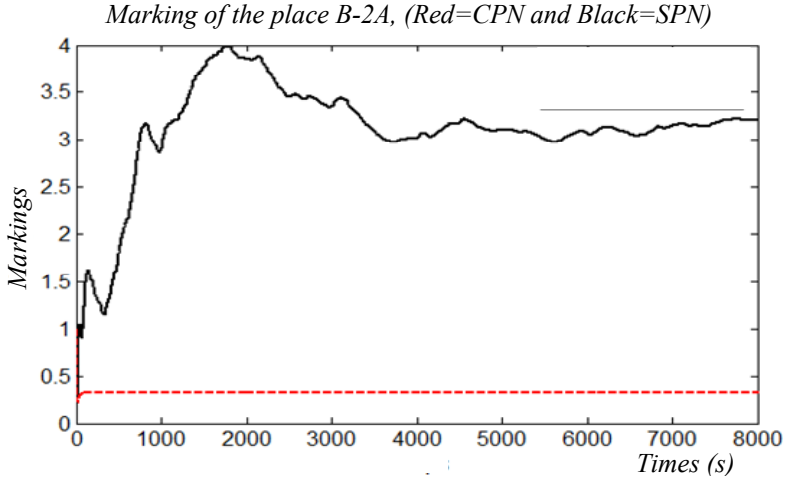

Figure 8 Flow evolution of CPN and SPN for transition *Out* in function of time of Figure 4

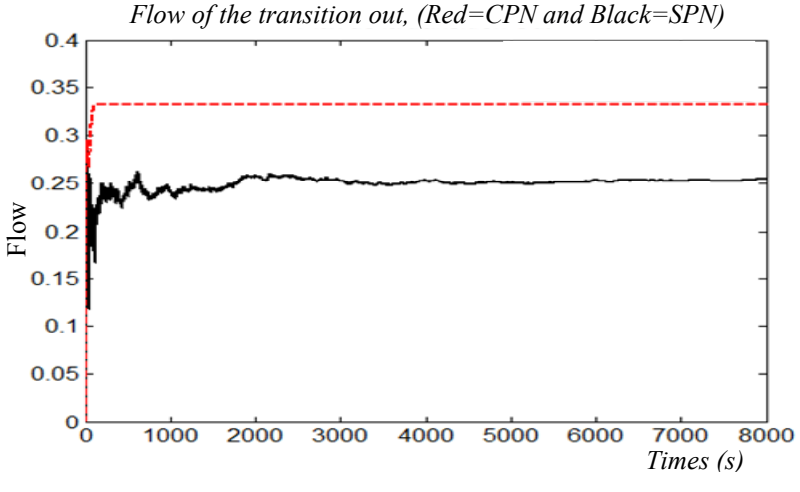

The results of the direct fluidification of the SPN of Figure 4 with $x_{\max j} = \mu_j$ of the place $B - 2A$ and the transition *Out* are grouped in the following table:

Table 3 Average flows and average markings of CPN and SPN from Figure 4 for $M_1 = (7\ 0\ 0\ 0\ 2\ 1\ 1\ 5\ 0\ 0\ 0\ 2\ 1\ 1\ 1\ 0\ 5\ 0)^T$

M_1= $(7\ 0\ 0\ 0\ 5\ 1\ 1\ 5\ 0\ 0\ 0\ 2\ 1\ 1\ 1\ 0\ 5\ 0)^T$	*SPN*	*CPN*	*Error*
Flows	0.2539	0.3333	0.31
Average markings	3.2083	0.3333	0.896

Finally, we illustrate the fluidification results of the SPN in Figure 4 with the initial labelling $M_1 = (35\ 0\ 0\ 0\ 10\ 1\ 1\ 25\ 0\ 0\ 0\ 10\ 1\ 1\ 1\ 0\ 25\ 0)^T$ and the same parameter. Figures 9 and 10 present, respectively the evolution of the marking of the place $B - 2A$ and the flow of the transition *Out*.

Figure 9 Marking evolution of CPN and SPN for place $B - 2A$ in function of time of Figure 4

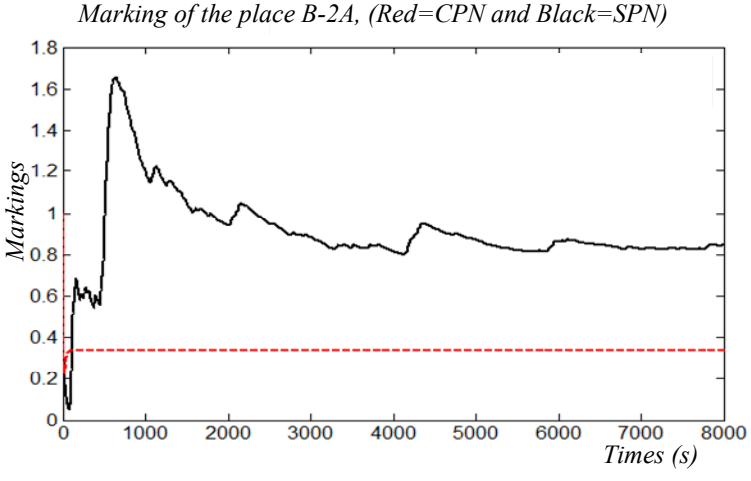

Figure 10 Flow evolution of CPN and SPN for transition *Out* in function of time of Figure 4

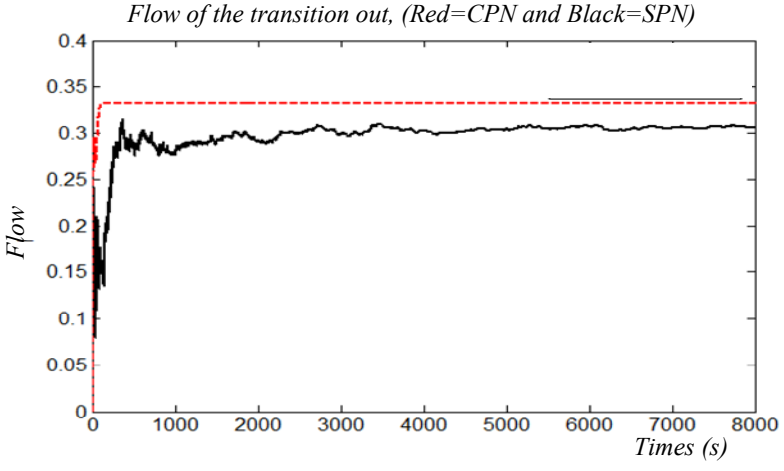

From Figures 9 and 10, we can see that the behaviour of the CPN obtained by the direct fluidification of the SPN with the same initial labelling does not converge towards the stochastic behaviour. Table 4 gathers the results obtained from the continuous and stochastic average marking of the place $B - 2A$ and from the continuous and stochastic average flow of the transition *Out*.

Table 4 Average flows and average markings of CPN and SPN from Figure 4 for $M_1 = (35\ 0\ 0\ 0\ 10\ 1\ 1\ 25\ 0\ 0\ 0\ 10\ 1\ 1\ 1\ 0\ 25\ 0)^T$

M_1= (35 0 0 0 10 1 1 25 0 0 0 10 1 1 1 0 25 0)^T	SPN	CPN	Error
Flows	0.32	0.33	0.039
Average markings	0.81	0.33	0.59

For different values of the initial marking, we can see that the trivial fluidification of the stochastic model described in Figure 4 under the infinite server semantics with the same structure and the same parameters of the PN leads to a CPN behaviour different from that of SPN. This difference is related to the presence of many synchronisations in the marking space of CPN, which induce many regions and in particular critical regions (Lefebvre et al., 2010) and the behaviour of the CPN depends on the critical place of each transition presenting a synchronisation. The behaviour of the CPN is non-linear due to the presence of the 'min' function (Lefebvre et al., 2010), this means that according to the markings of the places linked to a synchronisation, the CPN will not follow the same behaviour.

3.4 Regions in the reachability space

The system of Figure 4 contains 6 synchronisations at the level of the transitions *S*-M_1-*A*, *S*-M_2-*A*, *S*-M_2-*B*, *S*-M_1-*B*, *S*-M_3 and *E*-M_3. The several critical places of transitions presenting the several synchronisations. The marking space of the studied system is divided into 216 regions, of which 91 regions are reachable and 125 regions are empty, the different projections in the plane (*Pallets-B*, *Max-B*) of all the regions are represented in the following figure.

Figure 11 Reachability space of Figure 4

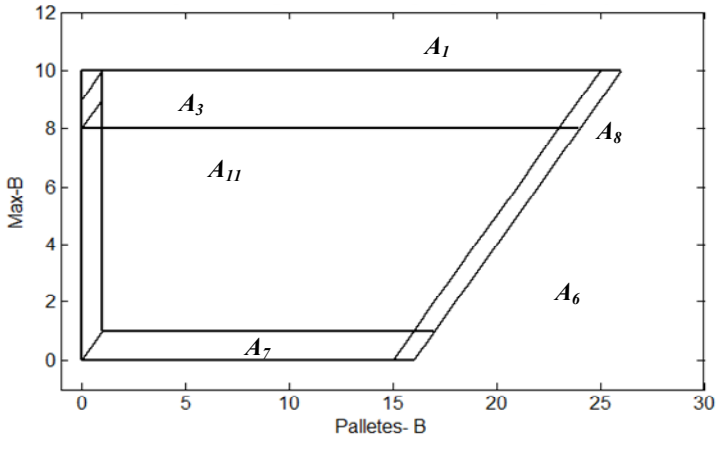

We will evaluate by simulation the distribution of the average asymptotic markings reachable by the SPN and CPN, for the same structure and the same parameters. The vector of the stochastic crossing rate and the maximum speeds of the continuous transitions are considered as random variables during the simulations, they are drawn according to a uniform probability distribution function (the simulation is carried out with 3000 random draws of the vector μ).

Figures 12 and 13 represent the distribution of average marking stochastic asymptotic and the continuous markings in the plane (*Pallets-B*, *Max-B*).

Figure 12 Asymptotic average markings with several firing rates of Figure 4

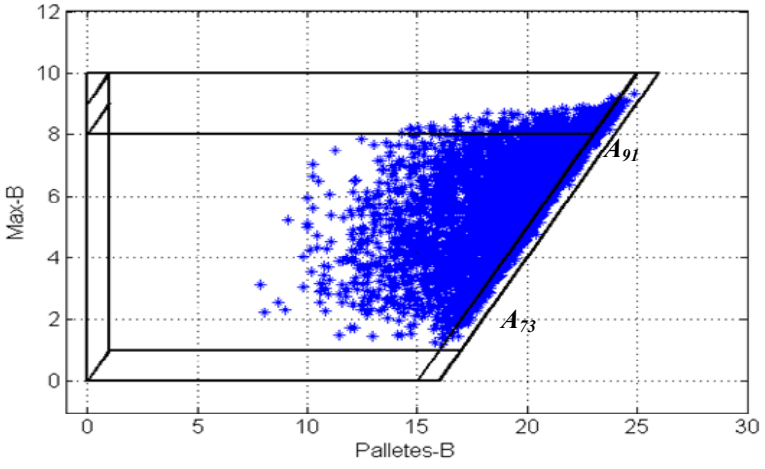

Figure 13 Asymptotic average markings with several crossing rates from Figure 4

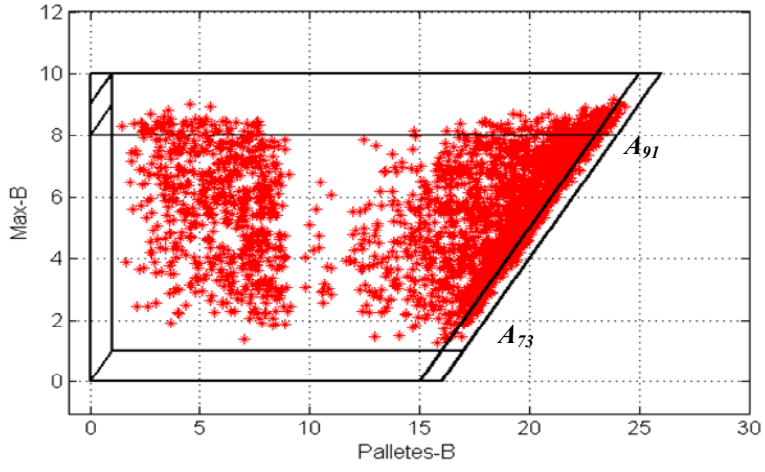

Given the values of SPN, initial marking and transition crossing rate. We find that the stochastic and continuous reachable regions are different in the same plane (*Pallets-B*, *Max-B*). To overcome the non-equivalence problem, we propose an adaptive approach

that adapts the maximum crossing rates of the continuous CPN by a corrective factor that is considered as a function of time, so that the modified CPN converges to the asymptotic stochastic marking.

3.5 Adaptive approach

In this part, we are interested in the approximation of SPN by CPN, whatever the initial marking. The notion of synchronisation is a key element of this approximation. More precisely, the presence of several regions and more particularly the existence of critical regions complicate the total direct fluidification of the SPN. In order to overcome this problem we will apply an approach called 'adaptive approach' is devoted to the adaptation of all the maximum crossing speeds of the CPNs by an adaptive corrector, these speeds considered as time dependent functions, so that the modified CPN converges to the SPN.

Equation (9) presents the adaptation law of the maximum speeds of crossing which is defined by the system of differential equations under the constraint $X_{\max} \geq 0$:

$$\dot{X}_{\max} = \eta.diag(\mu).\left(W^T\right).\left(M_s - M_c\right) + \left(X_s - X_c\right) \tag{9}$$

where $diag(\mu)$ is the diagonal matrix SPN firing rates, η is the adaptation parameter, $\left(X_s - X_c\right)$ represents the error related to the continuous and stochastic mean flows, and the vector $\left(M_s - M_c\right)$ the error due to variations in the stochastic and continuous mean markings.

Consider, for example the SPN described in Figure 4. This PN with initial marking $M_1 = \left(35\ 0\ 0\ 0\ 10\ 1\ 1\ 25\ 0\ 0\ 0\ 10\ 1\ 1\ 1\ 0\ 25\ 0\right)^T$ and of firing rate $\mu = \left(1\ 1\ 1\ 1\ 1\ 1\ 1\ 1\ 1\ 1\ 1\right)^T$ and of firing rate $\mu = \left(1\ 1\ 1\ 1\ 1\ 1\ 1\ 1\ 1\ 1\ 1\right)^T$ has a single firing invariant *T*-semi flow $z_1 = (1\ 1\ 1\ 1\ 1\ 1\ 1\ 1\ 1\ 1\ 1)^T$ and eight marking invariants. Therefore, only the flow of transition *Out* and the marking of the place $B - 2A$ will be considered. In order to have a continuous asymptotic regime converging towards that of the stochastic. We are going to apply the adaptation law defined by equation (9). Each crossing speed will be corrected by a multiplicative factor, and only the marking of the place $B - 2A$ and the flow of the *Out* transition will be represented.

Figure 14 represents the evolution of the average marking stochastic asymptotic and the modified continuous marking of the place $B - 2A$.

We can see in Figure 14 that the minimisation of the error due to the variations of markings over time allows the continuous average marking of the place $B - 2A$ to reach that of the average marking stochastic asymptotic of the same place.

Figure 15 represents the average continuous flow converges towards the stochastic flow of the *Out* transition, after the modification of the maximum speeds of the crossing of the continuous system.

Figure 14 Marking evolution of CPN and SPN place $B - 2A$ in function of time of Figure 4

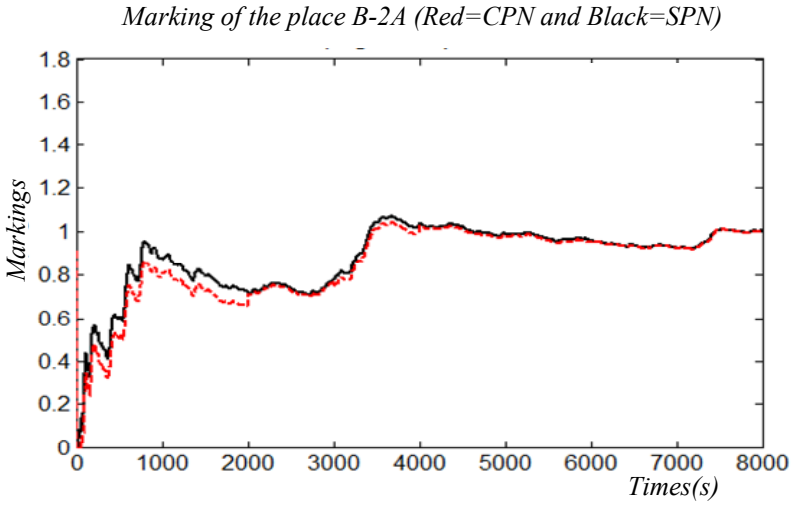

Figure 15 Flow evolution of CPN and SPN for transition *Out* in function of time of Figure 4

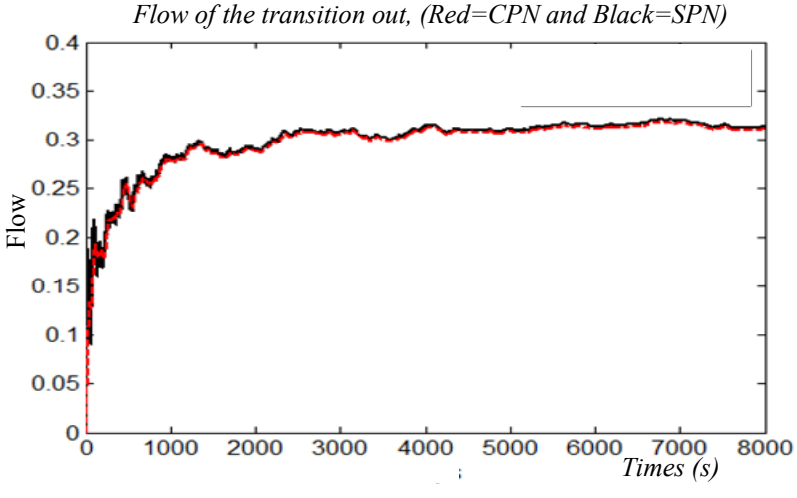

We modified the maximum speed of the *Out* transition using a multiplicative coefficient associated with each maximum speed of transition of the CPN, which depends on time, thus we note that the continuous average flow of the *Out* transition converges towards that of the system stochastic. The evolution of the correction coefficient associated with the maximum crossing speed of the *Out* transition as a function of time is represented in Figure 16.

Figure 16 Adaptation parameter evolution for transition *Out* in function of time of Figure 4

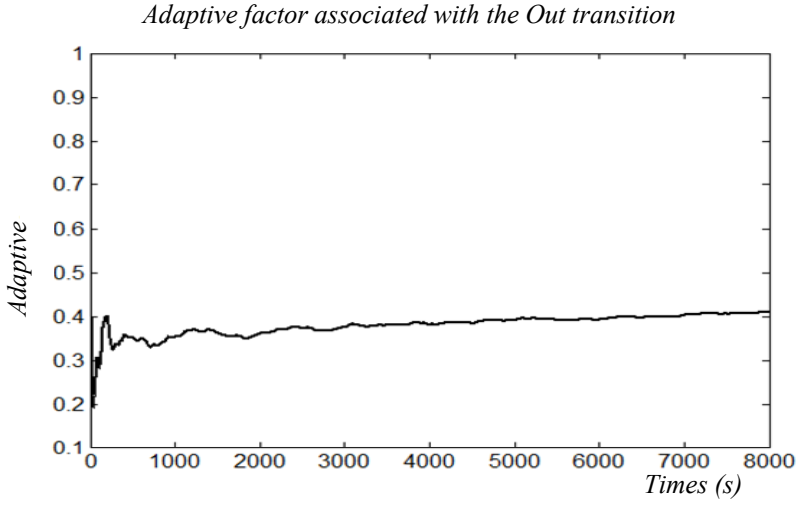

The modification of the maximum speeds using the correction coefficients applied to all the transitions of the CPN makes it possible to ensure the asymptotic convergence of the markings and the continuous average flows towards those of the stochastic. This approach requires knowledge of the mean marking stochastic asymptotic that one wishes to converge.

4 Conclusions

In this article, we have first presented the basic concepts of the different extensions of Petri nets, such as the SPN and the CPN. We exposed the limitations of the SPN, which is the slow convergence towards the stationary regime. We have shown that the CPN is a more interesting solution for estimating the average marking and flow of the SPN. Secondly, we have presented an example of a manufacturing workshop, in order to study the direct fluidification. This method preserves the structure of the network, the initial marking and the parameters of the transitions crossing. The CPN does not converge to the average marking and flow of the SPN in the long run. This is due to the existence of weighted edges and synchronisation. The presence of synchronisations leads to the division of the marking space into several regions, in particular the presence of the critical region. These two elements play an important role and limit the use of direct fluidification. This problem has been surmounted by using a numerical approach, which is characterised by maximum speeds of crossing adapted by an adaptive corrector. This corrector eliminates the errors due to the variations of the markings. Finally, we found that this approach gives better convergence to the stationary regime of the SPN.

The continuous model will be used to perform reliability studies as well as fault detection and diagnosis. In our future work, we will continue our research on the approximation of the steady state of the SPN by the faults of the continuous approaches directly related to the SPN and to the transition crossing speeds in order to obtain optimal alternative models.

References

Arzola, C., Ramírez-Treviño, A. and Silva, M. (2020) 'On the equilibrium sets of topologically equal conflict timed continuous petri nets', *IFAC-Papers Online*, Vol. 53, No. 4, pp.363–370.

Benaya, N., El-Akchioui, N. and Mourabit, T. (2018) 'Limits of fluidification for a stochastic petri nets by timed continuous petri nets', *International Conference on Intelligent Systems and Computer Vision (ISCV)*, IEEE, Morocco.

Benaya, N., El-Akchioui, N. and Mourabit, T. (2019) 'Approximation of stochastic petri nets by means of continuous petri nets: adaptive approach', *International Journal of Engineering and Technology*, pp.1–5.

Bobbio, A., Puliafito, A., Telek, M. and Trivedi, K. (1998) 'Recent developments in stochastic petri nets', *Journal of Circuits, Systems, and Computers*, Vol. 8, No. 1, pp.119—158.

Campos, J., Chiola, G. and Silva, M. (1991) 'Ergodicity and throughut bounds of Petri nets with unique consistent firing count vector', *IEEE Transactions on Software Engineering*, Vol. 17, No. 2, pp.117–125.

David, R. and Alla, H. (1992) *Petri Nets and Grafcet – Tools for Modelling Discrete Events Systems*, Prentice Hall, London.

El Akchioui, N. (2017) 'Fluidification of stochastic petri nets by no linear timed continuous petri nets', *American Journal of Embedded Systems and Applications*, Vol. 5, No. 4, pp.29–34.

El Akchioui, N., Dib, F., Lefebvre, D., Ncir, N., Sebbane, S. and Leclercq, E. (2020) 'About the fluifidication of SPN by CPN for complex dynamical systems: critical regions', *Proceedings of the 1st International Conference on Innovative Research in Applied Science, Engineering and Technology (IRASET)*, IEEE, Morocco.

El-Moumen, H., El Akchioui, N. and Zerrouk, M.H. (2022) 'Reliability analysis by Markov model and stochastic estimator of stochastic petri nets', *International Journal of Reliability and Safety*, Vol. 16, Nos. 1/2, pp.110–123.

El-Moumen, H., Nabil, E.A. and Zerrouk, M.H. (2023) 'Stochastic and continuous Petri nets approximation of Markovian model', *International Journal of Modelling, Identification and Control*, doi: 10.1504/IJMIC.2023.10057520.

Giua, A. and Silva, M. (2018) 'Petri nets and automatic control: a historical perspective', *Annual Reviews in Control*, Vol. 45, pp.223–239.

Júlvez, G., Recalde, L. and Silva, M. (2005) 'Steady-state performance evaluation of continuous mono-T-semiflow petri nets', *Automatica*, Vol. 41, No. 4, pp.605–616.

Lefebvre, D. (2011) 'About the stochastic and continuous petri nets equivalence in long run, non-linear analysis', *Hybrid Systems (NAHS)*, Vol. 5, pp.394–406.

Lefebvre, D. (2014) 'Fault diagnosis and prognosis with partially observed stochastic petri nets', *Proceedings of the Institution of Mechanical Engineers, Part O: Journal of Risk and Reliability*, Vol. 228, No. 4, pp.382–396.

Lefebvre, D. and Hadjicostis, C.N. (2022) 'Diagnosability of fault patterns with labeled stochastic petri nets', *Information Sciences*, pp.341–363.

Lefebvre, D., Leclercq, E. and Sanlaville, E. (2015) 'Tolerance intervals for stochastic processes with timed continuous petri nets', *IFAC-Papers Online*, Vol. 48, No. 3, pp.1018–1023.

Lefebvre, D., Leclercq, E., El Akchioui, N., Khalij, L. and Souza de Cursi, E. (2010) 'A geometric approach for the homothetic approximation of stochastic petri nets', *Proceedings of the IFAC WODES*, Berlin, Germany.

Lefebvre, D., Leclercq, E., Khalij, L., Souza de Cursi, E. and El Akchioui, N. (2009) 'Approximation of MTS stochastic petri nets steady state by means of continuous petri nets: a numerical approach', *Proceedings of the IFAC ADHS*, Zaragoza, Spain, pp.62–67.

Mahulea, C., Ramirez Trevino, A., Recalde, L. and Silva, M. (2008) 'Steady state control reference and token conservation laws in continuous petri nets', *Transactions on IEEE – TASE*, Vol. 5, No. 2, pp.307–320.

Molloy, M.K. (1981) *On the Integration of Delay and Troughput in Distributed Processing Models*, PhD, UCLA, Los Angeles, USA.

Molloy, M.K. (1982) 'Performance analysis using stochastic petri nets', *IEEE Transactions on Computers C*, Vol. 31, pp.913–917.

Navarro-Gutiérrez, M., Ramírez-Treviño, A. and Silva, M. (2016) 'Discontinuities and non-monotonicities in mono-T-semiflow timed continuous petri nets', *Proceedings of the 13th International Workshop on Discrete Event Systems (WODES)*, pp.493–500.

Navarro-Gutiérrez, M., Ramírez-Treviño, A. and Silva, M. (2022) 'Dual perspectives of equilibrium throughput properties of continuous mono-T-semiflow petri nets: firing rate and initial marking variations', *Automatica*, Vol. 136. Doi: 10.1016/j.automatica.2021.110074.

Rausand, M. and Hoyland, A. (2004) *System Reliability Theory: Models, Statistical Methods, and Applications*, Wiley, Hoboken, New Jersey.

Silva, M. and Recalde, L. (2002) 'Petri nets and integrality relaxations: a view of continuous petri nets', *Transactions on IEEE – SMC, Part C*, Vol. 32, No. 4, pp.314–326.

Silva, M. and Recalde, L. (2004) 'On fluidification of petri nets: from discrete to hybrid and continuous models', *Annual Reviews in Control*, Vol. 28, No. 2, pp.253–266.

Vazquez, R. and Silva, M. (2009) 'Hybrid approximations of Markovian petri nets', *Proceeding IFAC – ADHS*, Zaragoza, Spain, pp.56–61.

Vazquez, R., Recalde, L. and Silva, M. (2008) 'Stochastic continuous-state approximation of Markovian petri net systems', *Proceeding IEEE Conference on Decision and Control*, Cancun, Mexico, pp.901–906.